Received: 26 November 2024 | Accepted: 14 November 2025

DOI: 10.1002/2688-8319.70195

Ecological Solutions and Evidence

RESEARCH ARTICLE

Tracking plant condition in a functionally diverse restored plant community through a combination of proxy indicators

Jaume Ruscalleda-Alvarez[1,2,3] | Justin M. Valliere[2,4] | Victoria Marchesini[5] | Jason C. Stevens[2,3] | Jean W. H. Yong[2,6] | Erik Veneklaas[2]

[1]Commonwealth Scientific and Industrial Research Organisation (CSIRO), Waterford, Western Australia, Australia; [2]University of Western Australia, Crawley, Western Australia, Australia; [3]Department of Biodiversity, Conservation and Attractions, Government of Western Australia, Kensington, Western Australia, Australia; [4]University of California, Davis, California, USA; [5]Grupo de Estudios Ambientales, IMASL, Universidad Nacional de San Luis & CONICET, San Luis, Argentina and [6]Department of Biosystems and Technology, Swedish University of Agricultural Sciences, Alnarp, Sweden

Correspondence
Jaume Ruscalleda-Alvarez
Email: jaume.ruscalledaalvarez@csiro.au

Funding information
Australian Government Research Training Program; Australian Research Council Industrial Transformation Training Center for Mining Restoration, Grant/Award Number: ICI150100041; Argentinian National Research Sciences Council (CONICET)

Handling Editor: Péter Török

Abstract

1. Large-scale assessments of plant condition are needed in restored plant communities to evaluate if ecosystems are functioning similarly to natural reference systems. Remote sensing can yield information on plant condition in a more efficient way than current on-ground physiological methods, which often require destructive sampling and are difficult to perform at large scales. In this study, we explore the use of near-surface remote sensing approaches—leaf-level thermography and hyperspectral reflectance—to estimate key physiological parameters and track seasonal change in a diverse group of plant species growing in a restored mine site of Western Australia. In this system, deviations from expected plant condition are mainly driven by water availability, which translates in various degrees of drought stress.
2. We investigated the relationships between traditionally measured physiological variables and remotely sensed proxy indicators, with the following goals: (1) to assess the extent to which remotely sensed proxy indicators can reliably estimate key physiological variables in functionally diverse plant species, and (2) to explore a multivariate approach to track seasonal change in different species using a combination of remotely sensed proxy indicators.
3. Our results indicate that univariate relationships between physiological variables and their remotely sensed proxy indicator for leaf water content and total chlorophyll concentration were accurately predicted for all species at the leaf level. This was not the case for fluorescence and stomatal conductance. Through multivariate analysis, we found that, when grouping samples through seasonal data centroids, three different data sets (physiological variables, all remotely sensed proxy indicators and remotely sensed proxy indicators from hyperspectral reflectance

only) outlined very similar transitions across seasons in four out of the five studied species.
4. This indicates that, when combined, remotely-sensed proxy indicators generated through leaf hyperspectral reflectance have the potential to detect deviations in plant condition in a wide range of plant functional types. Using this approach to detect changes in levels of plant stress could enable early detection of potential issues in restoration and therefore may be used to inform adaptive management to improve long-term restoration strategy and outcomes.
5. *Practical implication*: through the multivariate approach based on remotely sensed proxy indicators that we present here, plant condition assessments can be conducted more efficiently in the context of ecological restoration.

KEYWORDS
ecological restoration, ecophysiology, hyperspectral reflectance, near-surface remote sensing, proxy indicators of plant condition, thermal imaging

1 | INTRODUCTION

Evaluating the performance of restored plant communities can yield useful information for assessing restoration success and informing appropriate interventions (Valliere et al., 2022). Assessing plant physiological condition can be conducted through well-established field or laboratory methods (Pearcey et al., 2012), resulting in high precision measurements. However, some of these methods can be difficult to perform in the field, especially for a large number of individual plants in short periods of time.

The limitations associated with large-scale physiological monitoring may be addressed by remote (or proximal) sensing-based methods. However, most current remote sensing developments in the context of ecological restoration focus on structural monitoring of plant community recovery (e.g. vegetation cover), with limited innovation in methods to measure plant physiological function (McKenna et al., 2020). Furthermore, ecosystem-level monitoring in the context of ecological restoration ignores the striking diversity of species and functional types, which is key to successful ecosystem processes and resilience (Walker et al., 1999). Therefore, there is a strong need for new monitoring methods that are able to provide insight into the performance of the diverse plant functional types present in a community.

Methods for plant condition assessment based on remote sensing have been studied, implemented and automated at various scales. Early applications include the determination of leaf chemical properties (Curran, 1989) and the determination of pigment content (Filella & Penuelas, 1994) and water status (Peñuelas et al., 1993), among others. More recently, increasingly complex approaches have been applied to high precision agriculture, phenotyping and glasshouse experiments, among others (Feng et al., 2021; Sishodia et al., 2020; Tao et al., 2022). Such methods have successfully detected differences in biomass, leaf area, leaf nitrogen content, leaf pigment content, leaf water status and transpiration rate, among others (Blackburn, 2006; Fu et al., 2021; Maes & Steppe, 2012; Rapaport et al., 2015; Siegmann & Jarmer, 2015; Thenkabail et al., 2019). In natural ecosystems, functional diversity of plant communities has been successfully retrieved from hyperspectral data (Asner et al., 2024; Serbin & Townsend, 2020; Townsend, 2014).

In this study, using a species-rich restored community, we test near-surface methods, as they provide the highest spatial, spectral and temporal resolution levels to validate relationships between key physiological traits and proxy indicators (numerical variables derived from remotely sensed data). Specifically, we use thermography to derive an indicator of plant water use, and hyperspectral reflectance to derive indicators of plant water status, pigment content and the condition of the photosynthetic apparatus.

We hypothesised that a combination of thermal and spectral information would be able to characterise plant condition change as reliably as traditionally measured physiological variables. We evaluated the use of these proxy indicators for vegetation monitoring in a recently restored Banksia woodland at a mine site in Western Australia. Through this study, we aim to contribute to the development of proximal and remote sensing tools that allow efficient gathering of quantitative and spatially explicit information on plant physiology to enhance our ability to monitor the performance of species and entire communities.

2 | MATERIALS AND METHODS

2.1 | Study site

The Hanson Construction Materials sand quarry is located on deep, siliceous Bassendean sand dunes, 30 km northeast of Perth, Western Australia. The climate is typically Mediterranean, with mild wet winters and hot dry summers. Air temperature and relative humidity at 0.5 m and rainfall were measured at 1-min intervals for the duration of the study from September 2018 to December 2019 (Figure 1).

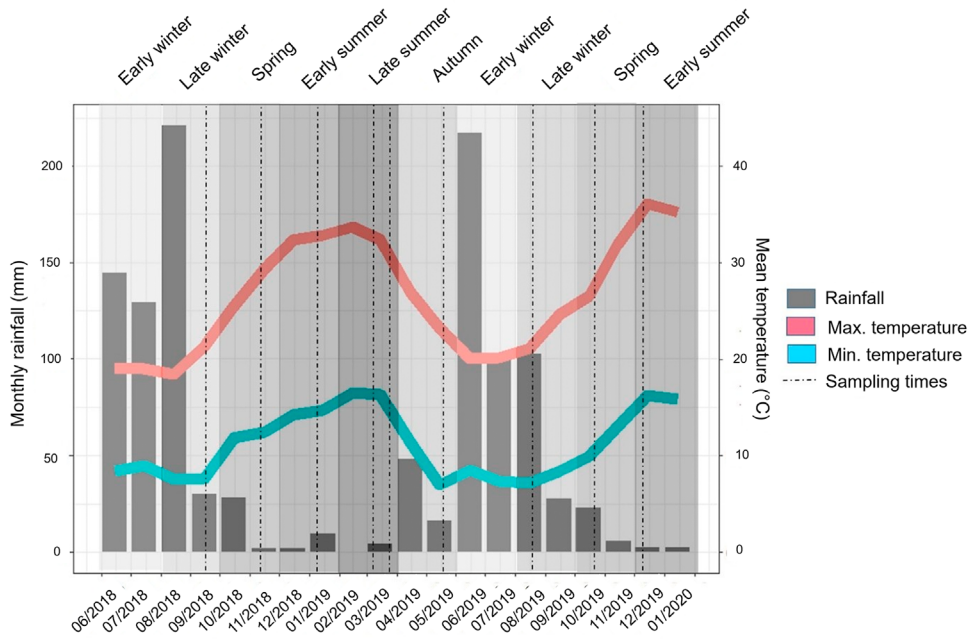

FIGURE 1 Monthly rainfall and mean minimum and maximum temperature in the study site, across different seasons and in relation to sampling times. Data prior to September 2018 were obtained from a weather station managed by the Australian Bureau of Meteorology located 7.1 km east of the study site.

TABLE 1 Studied species and respective adult form, leaf type, root system depth and stomata distribution.

Species	Family	Form	Leaf type	Root system	Stomatal distribution
Banksia menziesii R.Br.	Proteaceae	Tree	Broad	Deep	Lower side
Eucalyptus todtiana F.Muell.	Myrtaceae	Tree	Broad	Deep	Both sides
Jacksonia floribunda Endl.	Fabaceae	Shrub	Broad	Deep	Both sides
Hibbertia subvaginata (Steud.) F.Muell.	Dilleniaceae	Shrub	Narrow	Shallow	Both sides
Patersonia occidentalis R.Br.	Iridiceae	Herb	Broad	Shallow	Both sides

Note: Root system is classified as shallow (<2 m depth) or deep (>2 m depth) based on Pate and Bell (1999).

At the study site, a Banksia woodland plant community is being restored since 2016 following sand mining operations. Banksia woodlands are plant communities native to southwestern Australia (particularly the Swan Coastal Plain) with an overstorey dominated by Banksia species, along with some eucalypts and a species-rich understorey of sclerophyllous shrubs and perennial herbs (Pate & Beard, 1984). The five plant species chosen for this study (Table 1) are abundant at the study site and represent a wide variety of physiological functionality, in particular related to their adaptations to drought stress. Permits were granted by Hanson Construction Materials to carry out work in this site.

2.2 | Physiological monitoring

2.2.1 | Water use

On each sampling day, stomatal conductance (g_s) of one fully developed, recently matured leaf per plant was measured (on adaxial and abaxial leaf sides, to obtain a total g_s value in $mol_{water}\ m^{-2}\ s^{-1}$), between 8 am and 12 pm (although most measures took place between 9 and 11 AM), using a leaf porometer (SC-1, Decagon Devices, Pullman, WA, USA). Leaf water potential (LWP) assessments were conducted on the same leaves using a portable pressure chamber (Scholander PMS, Albany, OR, USA) between 11 AM and 2 PM.

2.2.2 | Water status

In the lab, leaf fresh weight (FW) was measured, and leaves were scanned with a metric reference for later calculation of leaf area with ImageJ software (Schneider et al., 2012). Leaves were incubated overnight at room temperature with their petiole submerged in de-ionised water in a dark container, and water-saturated fresh weight (SFW) was measured the following day. Leaves were then dried at 70°C for 48 h, after which dry weight (DW) was measured. From fresh, water-saturated and dry weight, relative water content

(RWC = (FW – DW)/(SFW – DW), $g\,g^{-1}$) and leaf absolute water content (LWC = (FW-DW)/FW, $g\,g^{-1}$) were calculated. From leaf area measurements and fresh and dry weights, equivalent water thickness (EWT = (FW – DW)/area) was calculated (in $g\,cm^{-2}$).

2.2.3 | Pigment content

One young fully developed leaf (or group of leaves in the case of *H. subvaginata*) of each plant was collected in every sampling campaign for pigment analysis. Samples were analysed for concentrations of chlorophyll a, chlorophyll b, total carotenoids and anthocyanins. Samples were dried and ground using a GenoGrinder (Horiba, Tokyo, Japan). Approximately 0.02 g of ground leaf tissue was weighed into 2 mL Eppendorf tubes, with the exact weight being recorded for each sample. For chlorophyll and carotenoid determination, 2 mL of cold 100% methanol was added to each tube, which were then vortexed and incubated overnight on a shaker at 4°C in darkness. Tubes were centrifuged at 14,000 rpm for 5 min to remove debris, after which 385 μL of supernatant were moved into the well of a microplate. Absorbance was measured at 470, 653 and 666 nm using a spectrophotometer (Hendry & Grime, 1993). For anthocyanin determination, another 0.02 g of ground leaf tissue was extracted as above in a separate 2 mL Eppendorf tube with 0.9 mL of cold acidified methanol. Centrifugation was done at 1000 rpm for 1 min, and 250 μL of supernatant was transferred into a well of the reading plate. Absorbance was measured at 530, 653 and 657 nm (Gould et al., 2000). Pigment concentrations (in $\mu g\,g^{-1}$dry sample) were calculated using standard formulas found in the literature for chlorophylls a and b and carotenoids (Hendry & Grime, 1993) and anthocyanins (Gould et al., 2000). Pigment concentration per dry weight was multiplied by leaf mass per area (LMA, $g\,cm^{-2}$) for each of the samples, to obtain pigment concentration per area of sample (in $\mu g\,cm^{-2}$).

2.2.4 | Photosynthetic efficiency

Finally, we also measured maximum potential quantum efficiency of Photosystem II (also referred to as *Fv/Fm* ratio) on young fully developed leaves of the same plants that were chosen for water status and pigment measurements. Leaves were dark-adapted for at least 20 min using leaf-clips and measures were taken with a chlorophyll fluorometer (Pocket PEA, Hansatech Instruments, Norfolk, UK). All measures were taken between 1 PM and 3 PM.

2.3 | Near-surface remote sensing monitoring

2.3.1 | Thermal imaging for stomatal conductance estimation

Prior to foliar conductance measurements, a thermal image was taken of the leaf using the dry reference leaf approach (Jones, 1999b). The thermal images including all three leaves were taken with an infrared camera (Fluke Ti 32, Everett, WA, USA) (see example of thermal image in Figure S1). Leaf temperatures were obtained by averaging temperatures of 10 points on each leaf through Fluke's SmartView 3.0 software, with emissivity set at 0.96 (value obtained in a preliminary experiment). In combination with data extracted from the minute-based meteorological data set, an equation following Jones (2014) was used to estimate stomatal resistance (Appendix S1, Equations S1–S5). While porometer-based stomatal conductance measures were taken throughout the entire study, thermal estimates of stomatal conductance were only conducted from May 2019 to December 2019 (in the last five sampling rounds), covering all seasons except late summer.

2.3.2 | Hyperspectral reflectance for water status estimation

Prior to LWP measures, leaf hyperspectral reflectance was measured with a spectroradiometer (ASD FieldSpec 4, Analytical Spectral Devices Inc., Longmont, CO, USA), using a leaf clip with an internal light source covering visible light region (VIS) to shortwave infrared light region (SWIR) wavelengths (300–2500 nm). Spectral data were exported using ASD software ViewSpecPro (Analytical Spectral Devices Inc., Longmont, CO, USA). Leaf-clip collected spectra were analysed in their raw state, from 450m to 2400 nm (350–450 nm and 2400–2500 nm regions were removed due to instrument noise).

Four different approaches were used to relate spectral data to physiological variables. The first approach explored normalised difference (ND) spectral indices using reflectance values at two different wavelengths R_1 and R_2 (Cao et al., 2015). ND indices are defined as $(R_2 - R_1)/(R_1 + R_2)$. All possible combinations of wavelengths were explored and correlated with the different water status variables. The wavelength combination that yielded the lowest root mean square error (RMSE) in the index-variable linear model was selected to build each one of the indices for further statistical testing.

The second approach analysed specific geometric aspects of water absorption spectral features (area, depth and depth/area in the reflectance curve) located in the near infrared (NIR) region, in particular at 970 and 1200 nm, and SWIR, specifically at 1450 and 1940 nm (Clevers et al., 2008).

In the third approach we quantified changes in reflectance within certain wavelength intervals (right and left slope of the 970 nm absorption feature and right and left slope of the 1200 nm absorption feature) within the water absorption features in the NIR region, all through linear ordinary least squares regression (Clevers et al., 2008, 2010). The second and third approaches were conducted in the R package hsdar (Lehnert et al., 2018).

Finally, we also used multivariate statistical analyses to consider all reflectance values of measured spectra, as well as subsets corresponding to different spectral regions separately (VIS, VNIR, NIR-SWIR and SWIR), through partial least squares regression (PLSR) (Serbin et al., 2014). Both absolute and derivative reflectance spectra were used within this approach. This was performed in the R package PLS (Wehrens & Mevik, 2007).

All models relating physiological variables with spectral traits were evaluated through the ratio of performance to deviation (RPD = standard deviation of the observed values/root mean square error of the model's predicted values) corresponding to validation data sets only (Bellon-Maurel et al., 2010). All RPD values presented in this study are an average of 100 values obtained by repeated random stratified sampling of calibration and validation data sets (in a 2/3–1/3 proportion). RPD was chosen as the preferred indicator of accuracy as it provides a dimensionless value of model prediction power on new data that is comparable across different physiological variables and different plant species (Williams, 2014).

2.3.3 | Hyperspectral reflectance for pigment content estimation

Hyperspectral reflectance was measured using a leaf clip (as described above) on the leaves that were collected for pigment content measures. For all five studied plant species and for all three main groups of pigments (total chlorophylls, carotenoids and anthocyanins) we conducted an optimised spectral index analysis. This was undertaken in the same way as conducted for plant water status determination (a normalised difference index in the form of $(R_2 - R_1)/(R_1 + R_2)$, where R_1 and R_2 are the reflectance values at two different 1 nm spectral bands, but restricted to pigment-relevant wavelengths only (400 to 800 nm)).

Upon determining that only total chlorophyll concentration (in $\mu g/cm^2$) could be reliably predicted for all studied species, we proceeded to identify a spectral index for chlorophylls that best suited all five species. For each species, we identified the range of R_1 and R_2 wavelengths that produced ND indices that in a simple linear regression would have coefficients of determination (R^2) higher than 90% of the maximum R^2 value obtained for that species. The middle points of these ranges were identified for each species, and these values were averaged to generate a spectral index that predicted total chlorophyll concentration accurately for all studied species. Analysis of covariance (ANCOVA) was performed to test the influence of species identity in determining different slopes in the relationship between chlorophyll content and the spectral index.

2.3.4 | Hyperspectral reflectance for photosynthetic efficiency estimation

Two different spectral indices were explored in a linear regression relationship with *Fv*/*Fm* measurements: the R_{740}/R_{800} index (Dobrowski et al., 2005) and the Double Peak Index (DPI) (Zarco-Tejada et al., 2003). In the latter case, and upon observing clear differences between species in terms of the location of this spectral feature, we determined average local maxima and minima through derivative analysis and used them to generate a species-specific DPI.

2.4 | Statistical analysis

2.4.1 | Univariate analysis

For all selected remotely sensed proxy indicators (estimated stomatal conductance, water status, pigment content and *Fv*/*Fm*), we conducted simple linear regression analyses with the corresponding measured physiological variables. All data management and statistical analysis were conducted in R (R Development Core Team, 2021).

2.4.2 | Multivariate analysis

We used multivariate statistics to track changes in plant condition across different seasons for each species according to different sets of variables. We grouped samples by season defined for the south-west of Western Australia.

Multivariate analyses were carried out in order to describe the seasonal changes in plant condition through multiple physiological variables including LWP, LWC, stomatal conductance, *Fv*/*Fm* and chlorophyll, carotenoid, and anthocyanin concentrations. Analyses were conducted for each species separately. Data distributions were evaluated for all variables for each species, and transformations (square root, logarithmic or fourth root) were applied as needed to meet statistical assumptions. Data sets were then normalised, after which the collinearity between all variables was assessed using Pearson's correlation. If the correlation coefficient between two variables was equal to or higher than 0.8, one of the two variables was removed from the data set (the one with a higher number of missing values). A similarity matrix between samples using Euclidean distances was built for each species. The differences in physiological variables between seasons were statistically tested using one-way permutational multivariate analysis of variance (PERMANOVA) with 9999 permutations. Upon determination of a significant seasonal effect, pairwise PERMANOVA was carried out to test which seasons were significantly different. The similarity matrices were visualised using non-metric multi-dimensional scaling (nMDS) plots. Additionally, the distance among season centroids was calculated from the Euclidean distance resemblances in order to locate the centre of each season's cloud of replicate points and project them into two-dimensional nMDS space to visualise seasonal change in plant physiology.

To examine whether remotely sensed proxy indicators can be used to track seasonal changes in plant condition in a similar way as done with physiological variables, the above multivariate analyses were repeated using remotely sensed proxy indicators. These remotely sensed proxy indicators were selected based on the strongest correlations between measured variables and proxy indicators. The best-performing indicators for a wide range of species included an estimated value of LWC (generated through PLSR), the DPI as a proxy for *Fv*/*Fm*, a chlorophyll spectral index as a proxy for total chlorophyll content and stomatal conductance estimated from thermal imagery through the dry reference method. To test whether the inclusion of thermal data significantly improved the capacity to track seasonal changes compared

to spectral data only, the multivariate analysis was done both with and without the thermal proxy of stomatal conductance.

The similarities between these three different multivariate approaches (physiological variables, all remotely sensed proxy indicators, and remotely sensed proxy indicators without thermal imagery data) were assessed through two different processes. First, we compared distances between season centroids obtained from two different data sets through a linear regression model. Secondly, we compared the relationships between the three resultant Euclidean centroid matrices from the separate data sets using Pearson's correlation. This procedure is described as a second-stage (2STAGE) analysis routine by (Clarke et al., 2014). The correlation coefficient matrices were visualised using nMDS.

The above multivariate analyses were conducted using the software PRIMER 7 (v. 7.0.13, https://www.primer-e.com/). All figures were produced using RStudio (v.1.0.143, https://rstudio.com/) (R Core Team, 2021). All data used for this analysis were collected under an agreement between the ARC Centre for Mine Site Restoration and Hanson Construction Materials and are available at Dryad (Ruscalleda-Alvarez, 2026).

3 | RESULTS

3.1 | Univariate relationships between physiological variables and near-surface proxy indicators

Leaf water content (Figures 2 and 3) and total chlorophyll concentration (Figure 4) were accurately predicted for all studied species. This was not the case for fluorescence (Figures 5 and 6), stomatal

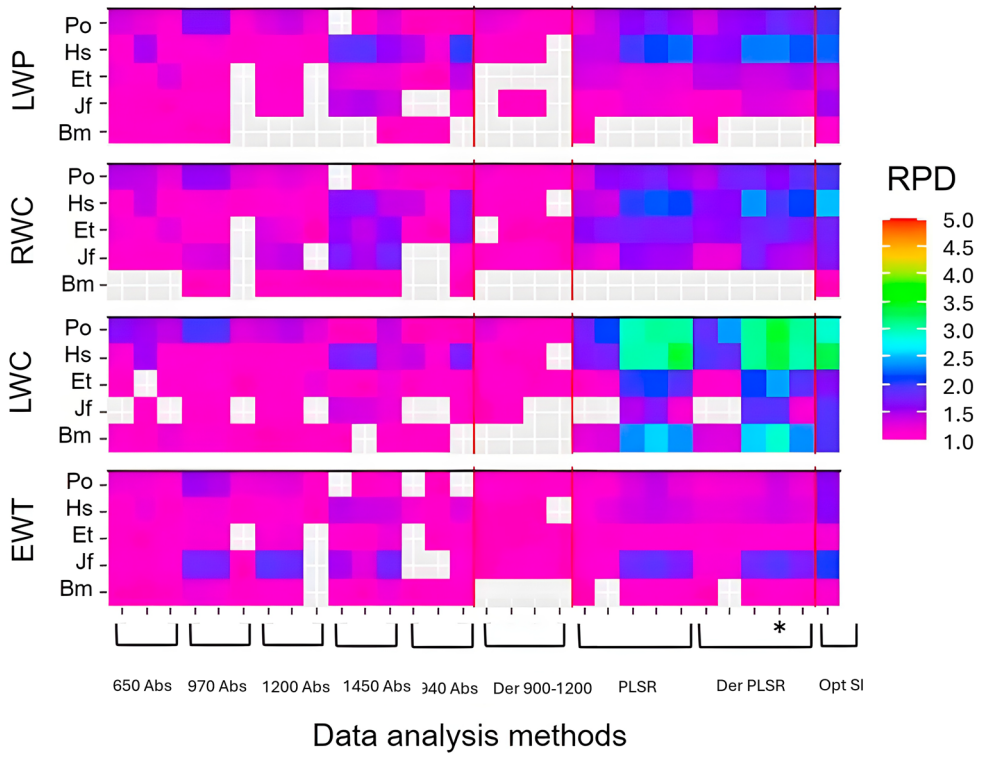

FIGURE 2 Ratio of performance to deviation (RPD) values (from validation data set) for each of the methods studied, for all species and for different variables related to plant water status and water content (LWP: leaf water potential, RWC: relative water content, LWC: leaf water content, EWT: equivalent water thickness), using leaf level spectral signatures. Only RPD values above 1 are presented. Species abbreviations: *Banksia menziesii* (Bm), *Jacksonia floribunda* (Jf), *Eucalyptus todtiana* (Et), *Hibbertia subvaginata* (Hs) and *Patersonia occidentalis* (Po). On the *x* axis, spectral analysis method grouping (in brackets) and specific methods used in these groups (represented by individual ticks within each group). From left to right the first five groups represent water absorption features: 650 nm absorption feature (650 Abs), 970 nm absorption feature (970 Abs), 1200 nm absorption feature (1200 Abs), 1450 nm absorption feature (1450 Abs) and 1940 absorption feature (1940 Abs). In each absorption feature there are three ticks that indicate three different measures: area of the absorption feature, maximum depth of the absorption feature and maximum depth/area of the absorption feature. Derivative reflectance features between 900 and 1200 nm (Der 900–1200), which includes, from left to right, the following measures: slope of the spectrum between 900 to 970 nm, 1000 and 1050 nm, 1100 and 1200 nm and 1200 and 1270 nm), partial least square regression (PLSR) using absolute reflectance, using the visible spectrum only (450 to 700 nm), visible and near infra-red spectrum (450 to 950 nm), near infra-red and shortwave infra-red spectrum (700 to 2400 nm) and shortwave infra-red spectrum (950 to 2400 nm), partial least square regression using derivative reflectance (derPLSR), using the same methods described for absolute reflectance), optimised spectral indices (Opt SI) in the form of a normalised difference index, $(R_2 - R_1)/(R_1 + R_2)$, where R_2 and R_1 are two different 1 nm wide wavelengths). On the horizontal axis, the method marked with '*' represents the best performing method across a larger number of species (PLSR using derivative shortwave infrared reflectance).

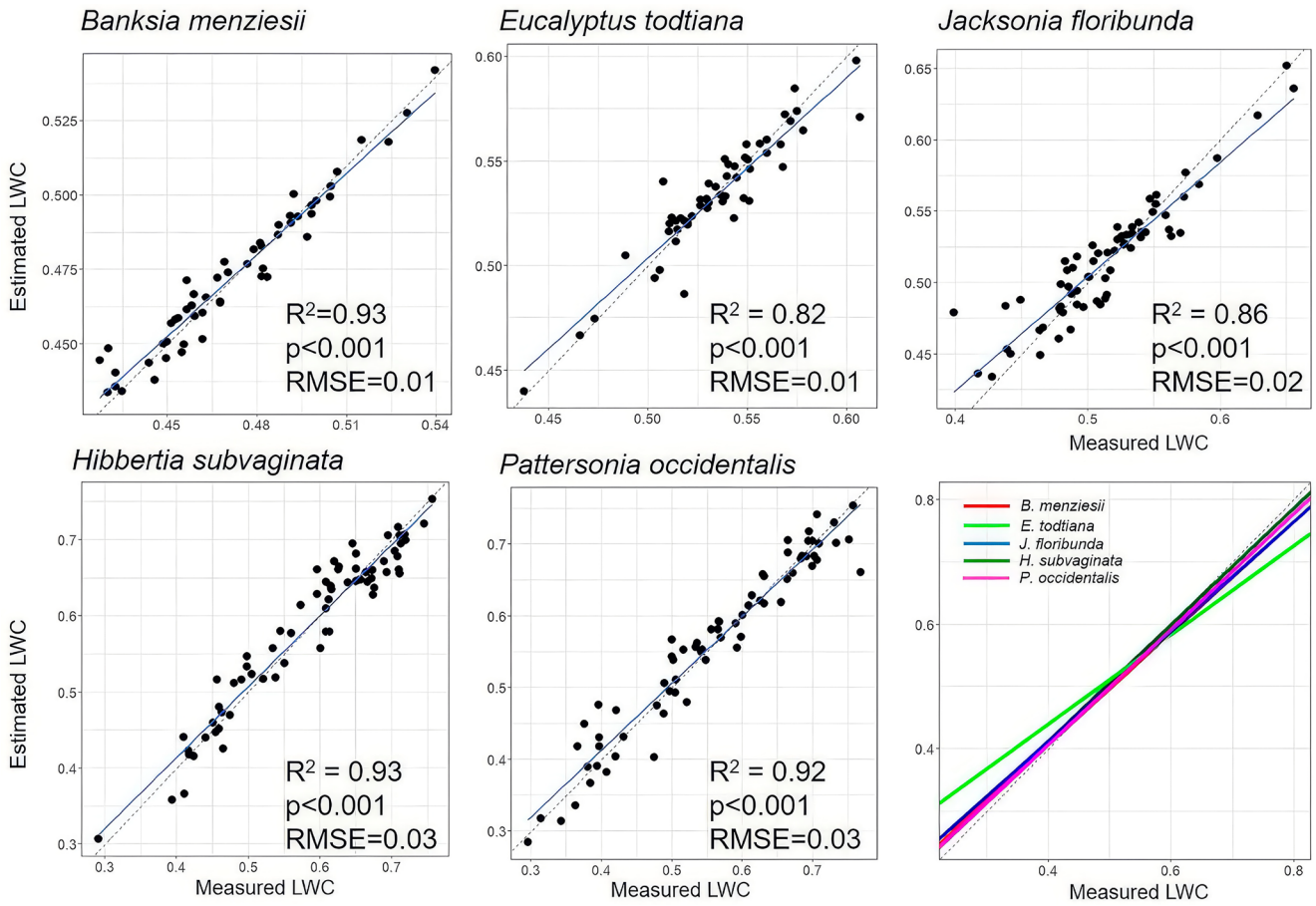

FIGURE 3 Estimated and measured values of leaf water content (LWC) in all studied species, using partial least square regression through shortwave infrared derivative reflectance (all samples included). A linear model was fitted to these data (blue line), and R^2, *p*-value and root mean square error (RMSE) are presented in each plot. Dotted line represents a 1:1 relationship between measured and estimated values. The lower-right panel represents the linear fitted model for each species with respect to the 1:1 relationship.

conductance (Figure 7), carotenoids and anthocyanins (Table S3.3). As a summary, all coefficients of determination of linear regressions corresponding to the univariate relationships studied are presented in Table 2. Note that while partial least squares regression is technically a multivariate statistics method, we are including it under the univariate methods not to confuse the reader with the multivariate approach presented in the following section (where several variables are combined in a non-metric multi-dimensional scaling approach).

Further detail on univariate relationships between ecophysiological variables and near-surface proxy indicators, as well as ecophysiological variation observed, can be found in the Supporting Information. These include (1) seasonal variation of physiological variables tracked during the study (Figures S2.1 and S2.2), revealing expected functional diversity in a Banksia woodland, (2) optimal wavelength ranges to generate a spectral index that correlates well with area-based chlorophyll content for all studied species (Table S3.1), which shows how an optimised spectral index was generated to predict chlorophyll content using reflectance at 714 and 758 nm; and (3) ANCOVA analysis of the interaction effect between species and the slope of the index value – chlorophyll content relationship (Table S3.2), which reveals that the relationship between the multi-species optimised index and area-based chlorophyll content is different according to species, (4) water status spectral analysis method and model accuracy (Figure S4), which shows that leaf water content is the variable better predicted across species using PLSR and optimised spectral indices, and (5) coefficients of determination, root mean square error (RMSE) and wavelengths selected for the formation of an optimised spectral index that would provide the lowest RMSE of linear models predicting a set of water status-related variables (Table S7).

3.2 | Multivariate analysis

3.2.1 | PERMANOVA

PERMANOVA results revealed that season had a highly significant effect on observed changes in physiological variables of all species (Table S5.1). The level of significance was the same ($p < 0.001$) irrespective of the inclusion of estimated stomatal conductance from thermal imagery.

PERMANOVA results for the two sets of proxy indicators were identical because estimated stomatal conductance from thermal

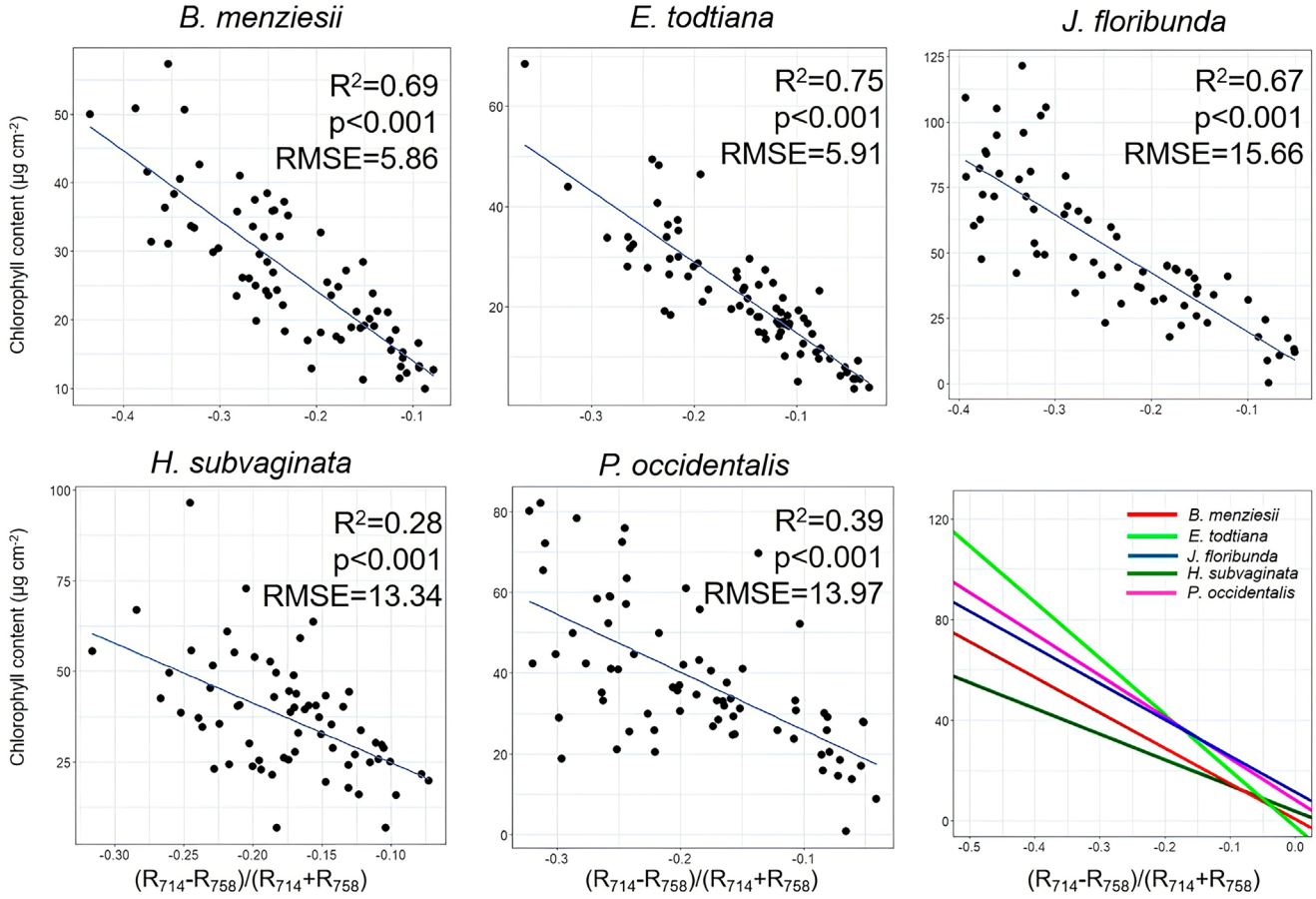

FIGURE 4 Linear regressions between total chlorophyll content and the spectral index $(R_{714}-R_{758})/(R_{714}+R_{758})$. R^2, p-values and root mean square error (RMSE) are presented in each plot. The lower-right panel represents the linear fitted model for each species.

imagery data was highly correlated with estimated LWC (Pearson's $r>0.8$) and therefore removed from the analysed data set. Pairwise PERMANOVA results highlighted the high degree of similarity between the seasonal patterns apparent in the physiological data set and the remotely sensed data sets (Table S5.2).

3.2.2 | Non-metric multi-dimensional scaling

Non-metric multi-dimensional scaling (nMDS) using physiological variables revealed that *Fv*/*Fm*, chlorophyll content, stomatal conductance, LWC and LWP were the most influential variables in separating late winter and spring samples from early and late summer samples which clustered together in the ordination (Table S5.3). However, the influence of each one of these variables depended on the species (Figure 8 and Figure S6). The *Fv*/*Fm* ratio was an important variable for tracking seasonal change for all species, as was LWP for all species except *B. menziesii*. Chlorophylls and stomatal conductance had an almost identical influence when separating samples from periods with greater or lower water availability for *B. menziesii*, *E. todtiana* and *J. floribunda*, whereas that was not the case for the most anisohydric species *H. subvaginata* and *P. occidentalis*.

In the analysis using all proxy indicators, the chlorophyll spectral index, and to a minor extent estimated stomatal conductance, explained seasonal separation in *B. menziesii* and *E. todtiana* (Figure 8 and Figure S6). In the case of *H. subvaginata* and *P. occidentalis*, the two variables that explained the separation of samples from different seasons were the DPI and estimated LWC, whereas for *J. floribunda* it was the DPI only.

When omitting estimated stomatal conductance from the group of proxy indicators, the chlorophyll spectral index became the variable that best separated samples of different seasons for *B. menziesii* and *E. todtiana* (Figure 8 and Figure S6). The DPI was the most influential variable for *J. floribunda* and *P. occidentalis*. In the case of *H. subvaginata*, the variable selection process carried out using the full proxy-derived data set left out estimated conductance, so this step was not necessary.

For all species and with all data sets, the season centroids within the nMDS space showed a transition between early summer and late summer, through autumn, towards the late winter and spring centroids (Figure 8 and Figure S6). However, the distances between centroids varied by species. For example, for *B. menziesii* and *E. todtiana*, the early summer and late summer centroids were closer to each other compared to those of *J. floribunda*, *H. subvaginata* and *P. occidentalis*.

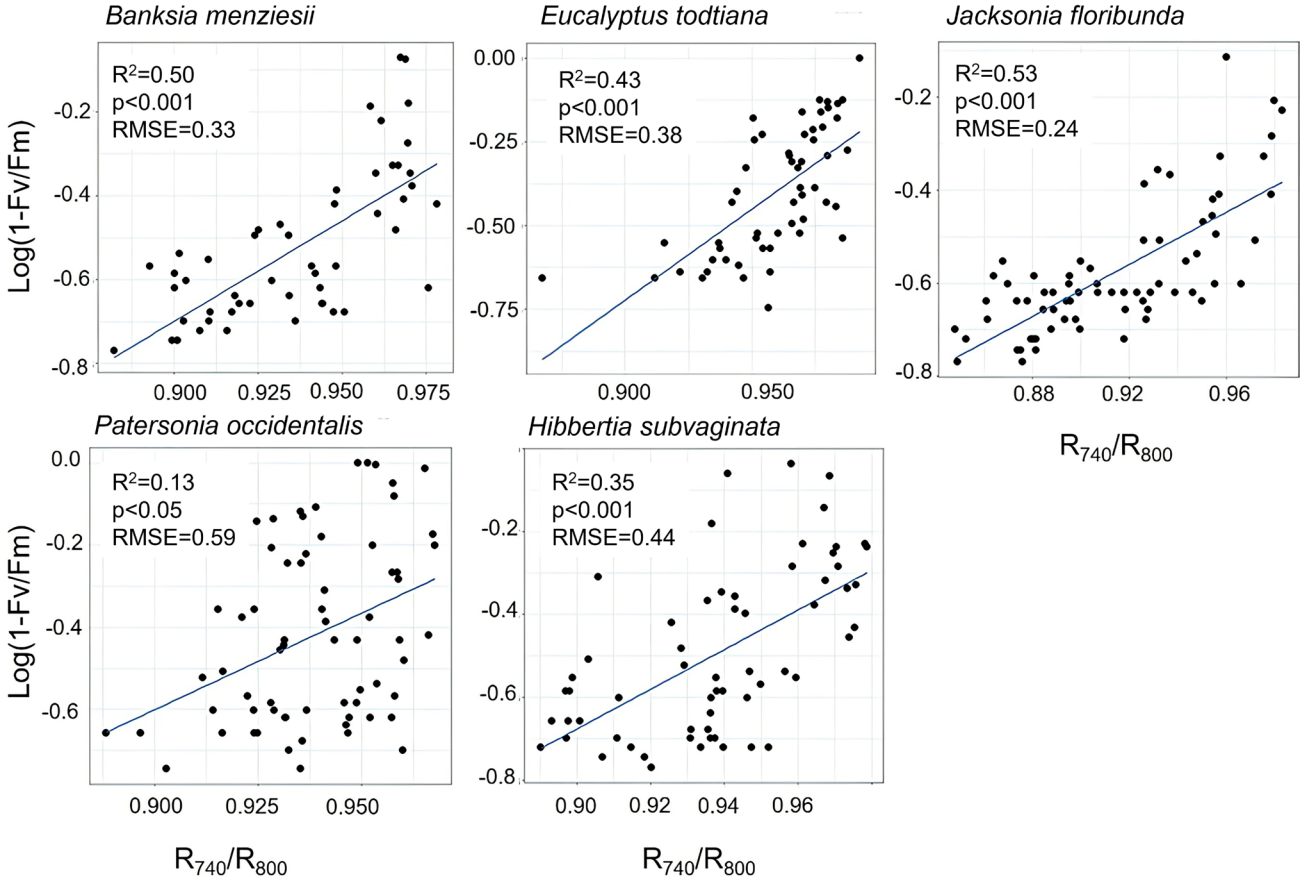

FIGURE 5 Linear regression relationships between chlorophyll fluorescence (*Fv*/*Fm*) and the R_{740}/R_{800} index (in a log-transformed format) for all studied species. R^2, *p*-values and root mean square error (RMSE) are presented in each plot. RMSE has been calculated to represent *Fv*/*Fm* values and not the transformed value presented in the *y*-axis.

Direct comparisons of distances between seasons using both the physiological data set and the full proxy variable data showed strong correlations (R^2 between 0.76 and 0.93; $p < 0.05$) in all species except *J. floribunda* (Figure 9 and Figure S6). Removing estimated conductance from the proxy variable data set did not substantially change this pattern in any of the species. A summary figure (Figure 9) outlines the relationships between season centroids using physiological and proxy-derived distances (without thermal data) for all five studied plant species.

3.2.3 | Second stage nMDS

Second stage non-metric multi-dimensional scaling (2STAGE nMDS) is a type of plot that allows for the visualisation of the similarity between two correlation matrices. In these plots, the closer two points are to each other, the more similar the season centroid distance matrices they represent are. The seasonal centroid matrices based on physiological variables and on all proxy indicators for *H. subvaginata* and *P. occidentalis* were closely plotted, indicating that seasonal patterns of those two species derived by those two data sets were highly correlated to each other. In contrast, *J. floribunda* showed the largest distance between overall season centroid resemblance matrices, indicating that the seasonal patterns explained by the two data sets corresponded less accurately to each other. Relatively small distances for *B. menziesii* and *E. todtiana* indicated greater correspondence between physiological and proxy data sets than for *J. floribunda*, but not as strongly as for *H. subvaginata* and *P. occidentalis*.

The analysis of 2STAGE nMDS between season centroid resemblance matrices showed very similar results for *P. occidentalis*, *B. menziesii* and *E. todtiana*, and larger differences for *J. floribunda* (Figure 10). This analysis was done using the physiological variable data set and the proxy-derived variable data set without estimated conductance. Finally, 2STAGE nMDS analysis between season centroid resemblance matrices showed very similar results for *B. menziesii*, *J. floribunda* and *P. occidentalis*, whereas *E. todtiana* showed a larger difference between season characterisation using two different data sets. Those data sets were the proxy-derived variable data set with all variables and the proxy-derived variable data set without estimated conductance.

4 | DISCUSSION

Our results demonstrate that combinations of remotely sensed indicators of physiological variables can reliably mirror plant physiological

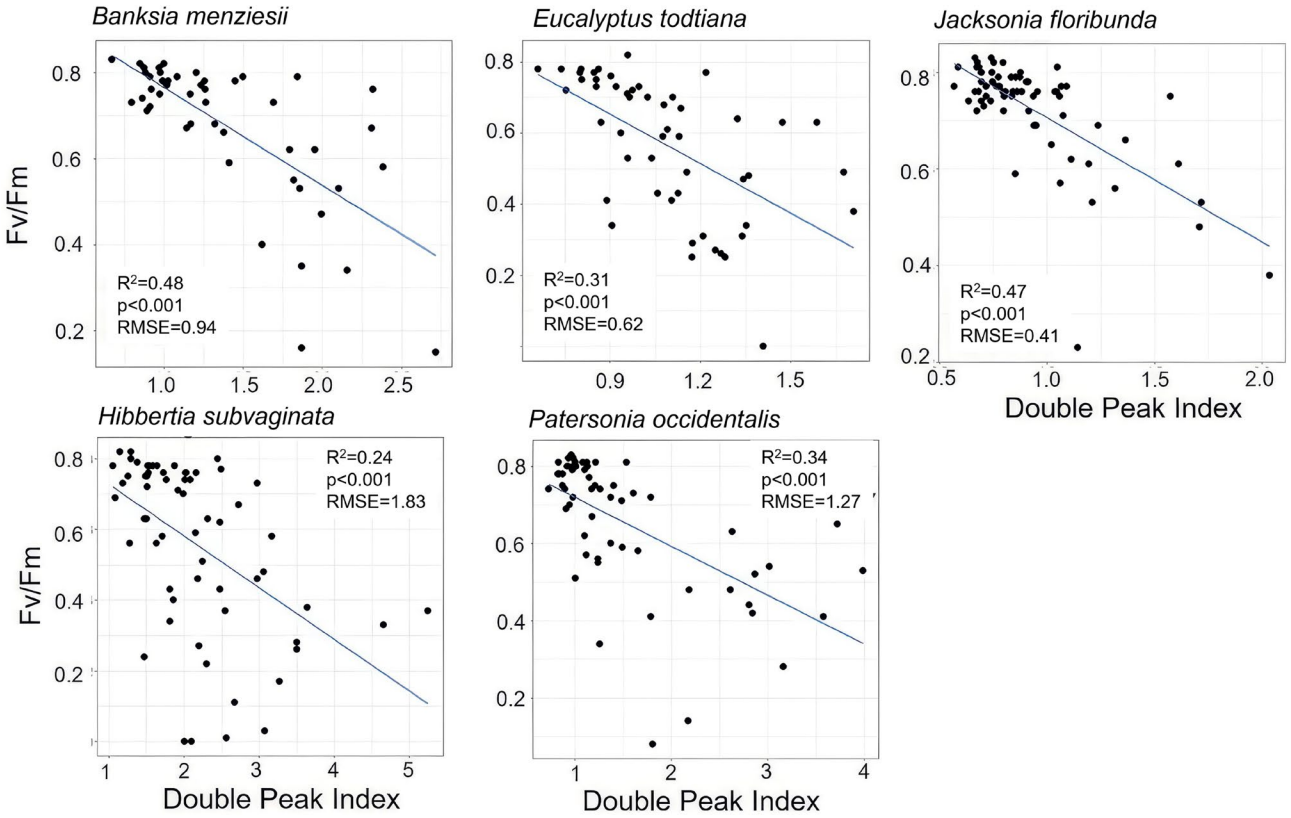

FIGURE 6 Linear regression relationships between chlorophyll fluorescence (*Fv/Fm*) and the species-specific Double Peak Index (DPI) for all studied species. R^2, *p*-values and root mean square error (RMSE) are presented in each plot.

condition in a seasonally stressful environment across functionally diverse species. While prediction of single physiological variables through remotely sensed indicators was expected, it was not always robust (i.e. relatively low accuracy and interspecific inconsistencies). However, a multivariate approach showed great promise, presumably due to the greater information content and the fact that species differ in how strongly they express adaptive traits. Despite the importance of drought as a stressor, thermal sensing (an indicator of transpiration rate) did not contribute sufficiently to the multi-trait analysis to warrant its inclusion, which suggests that spectral-only sensing is adequate for monitoring plant condition. From a practical point of view, the multivariate method we present here could allow for more efficient monitoring of plant condition compared to traditional eco-physiological methods.

4.1 | Univariate relationships

4.1.1 | Thermal assessment of water use

Thermal imagery analysis based on the dry reference method yielded highly significant relationships between measured and estimated stomatal conductance for all species, as expected from studies conducted on crop species (Jones, 1999a; Leinonen et al., 2006). Although stomatal conductance was overestimated for all species, to different extents, comparisons of estimated conductance of target plants and reference plants would still reflect (relative) differences in actual stomatal conductance. Overestimation of stomatal conductance may be partly due to inaccuracies in the measurement of air and leaf temperature or VPD, but tests conducted under controlled conditions (Ruscalleda-Alvarez, 2022) suggest that complexities associated with the estimation of boundary layer conductance also play a large role. In the field, boundary layer conductances are very difficult to measure, due to continuously varying wind speeds within vegetation. Moreover, many leaf types (e.g. small, non-flat, clustered) are aerodynamically quite distinct from the simple flat or circular objects that most theory is based on (Monteith & Unsworth, 2013). Accurate thermal sensing of stomatal conductance for ecological purposes will therefore remain challenging due to the variability of in-canopy microclimates and complexity of boundary layer effects. Our results, however, indicate that it is a very useful non-contact method to compare differences in transpiration rate between plants of the same species, even under challenging field conditions.

4.1.2 | Leaf water status

Accuracy of leaf water status predictions differed considerably among the physiological variables assessed. LWC was very accurately determined in four out of the five studied species through

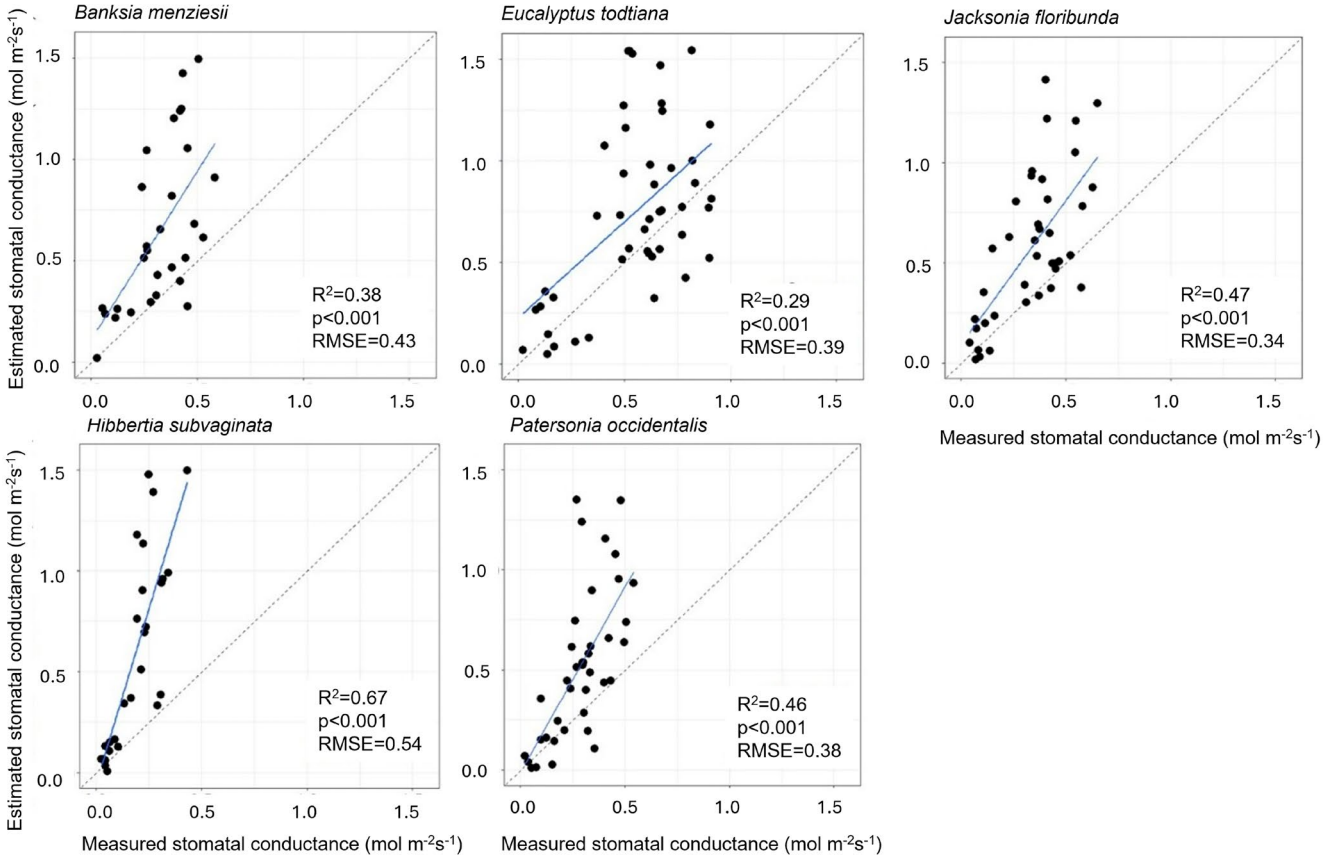

FIGURE 7 Stomatal conductance (g_s) of the five studied species measured using a porometer and estimated using thermal sensing. A linear model was fitted to these data (blue line), and R^2 and *p*-value are presented in each plot. Dotted line represents a 1:1 relationship between measured and estimated values.

TABLE 2 Coefficients of determination of linear regressions corresponding to univariate relationships between measured and estimated physiological variables.

	Estimated conductance	Leaf water content	Total chlorophyll content	Total carotenoid content	Total anthocyanin content	Fv/Fm
B. menziesii	0.38	0.93	0.69	0.17	0.15	0.50
E. todtiana	0.29	0.82	0.75	0.17	0.15	0.43
J. floribunda	0.47	0.86	0.67	0.07	0.08	0.53
P. occidentalis	0.46	0.92	0.39	0.28	0.42	0.35
H. subvaginata	0.67	0.93	0.28	0.39	0.15	0.13

Note: Estimated conductance calculated through dry-reference energy balance equations; leaf water content estimated through Partial Least Square Regression of shortwave infrared derivative reflectance; total chlorophyll content estimated through a normalised difference optimised spectral index common for all species; total carotenoids and anthocyanins content estimated through species-specific normalised difference optimised spectral indices; Fv/Fm estimated through the R_{740}/R_{800} spectral index.

PLSR using SWIR derivative reflectance. However, this method had to be optimised for each species separately. Model accuracy was particularly high for anisohydric species which showed large changes in LWC through the seasons, including *H. subvaginata* and *P. occidentalis*. The predictive value of SWIR is expected since leaf water dominates the spectral signature of leaves in this spectral region (Curran, 1989), and LWC is essentially the concentration of water molecules in the leaf tissue. Vegetation water indices have been known for decades and have traditionally been based on spectral band ratios within NIR and SWIR regions (Peñuelas et al., 1993; Sims & Gamon, 2003). However, in this study we have found that hyperspectral data analysed through a multivariate approach such as PLSR provided better predictions of LWC than 2-band indexes tested through all possible band combinations within the visible, NIR and SWIR ranges. This is consistent with other studies that have found the PLSR analysis of hyperspectral

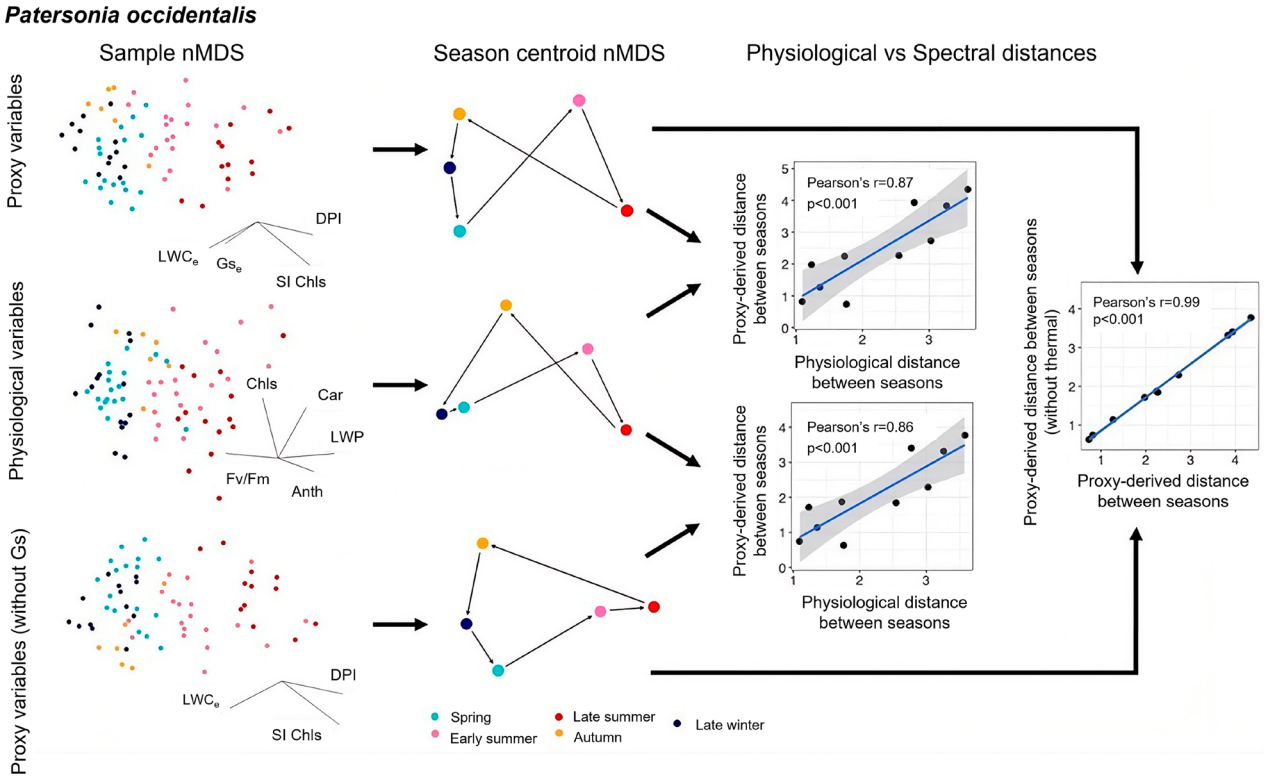

FIGURE 8 Non-metric multidimensional scaling (nMDS) using Euclidean Distance of physiological (middle) and proxy variable with (top) and without estimated conductance Gs (bottom) for *Patersonia occidentalis* (other species'figures provided in the appendices section). Vectors in the bottom right of each sample nMDS plot represent the Pearson correlation of variables explaining the variation. Vector directions and lengths indicate the relative influence of each variable in separating samples within the multi-dimensional space. Season centroids nMDS were produced from the distance among centroid for each season, calculated from the Euclidean distance resemblances. Scatterplots (right) show the relationship between the Euclidean distances matrices of the seasonal centroids derived from two data set. Blue line and grey area represents the linear relationship and 95% confidence interval, respectively. Each point in the scatter plot represents a Season 1–Season 2 comparison. Anth, total anthocyanin concentration; Chls, total chlorophyll concentration; DPI, Double Peak Index, Car, total carotenoids concentration; Gs, stomatal conductance; Gs_e, estimated stomatal conductance; LWC, leaf water content; LWCe, estimated leaf water content; SI Chl, spectral index related to chlorophyll content.

data to accurately predict water status (Lu et al., 2024; Rapaport et al., 2015), In contrast to LWC, LWP is a measure of the energy status of water in the plant tissue (in pressure units), which is not only related to water concentration but also to osmotic and elastic properties of the tissue (Lambers et al., 2008), and has no direct physical relationship with leaf spectral properties. Our observation that RWC (which is the ratio between actual LWC and LWC at saturation) did not correlate as well with spectral data as LWC did, suggests that there was considerable variation in the saturated value of LWC. Finally, no significant relationships were found between EWT and any of the spectral indicators of water status. We hypothesise that leaf reflectance for these species was mostly determined by leaf epidermal properties, and that limited penetration of the relevant wavelengths into the leaves limits the ability to sense the 'depth' of water in the leaf. In conclusion, spectral indices correlate more strongly with LWC than with RWC, EWT or LWP, because LWC is most closely related to the probability that incident radiation hits a water molecule near the leaf's surface. Although LWC differs strongly among species and is not as informative for plant physiology as LWP and RWC, changes in LWC within a species can be a useful indicator of dehydration in response to drought stress.

4.1.3 | Chlorophyll content

The red edge spectral region (between 690 and 800 nm) was particularly informative of total chlorophyll content, as expected (Filella & Penuelas, 1994). This was the case in all the studied species, which represent a variety of leaf morphologies and sizes. The two species for which regression coefficients for total chlorophyll determination were lower (*H. subvaginata* and *P. occidentalis*) were also the two species with higher concentrations of carotenoids and anthocyanins. These other pigments will have influenced the reflectance of the wavelengths used for chlorophyll estimation (Vina & Gitelson, 2011), especially if they were present closer to the leaf surface than the chlorophyll. Overall, our results show that total chlorophyll content can be accurately predicted for a wide diversity of species (both in

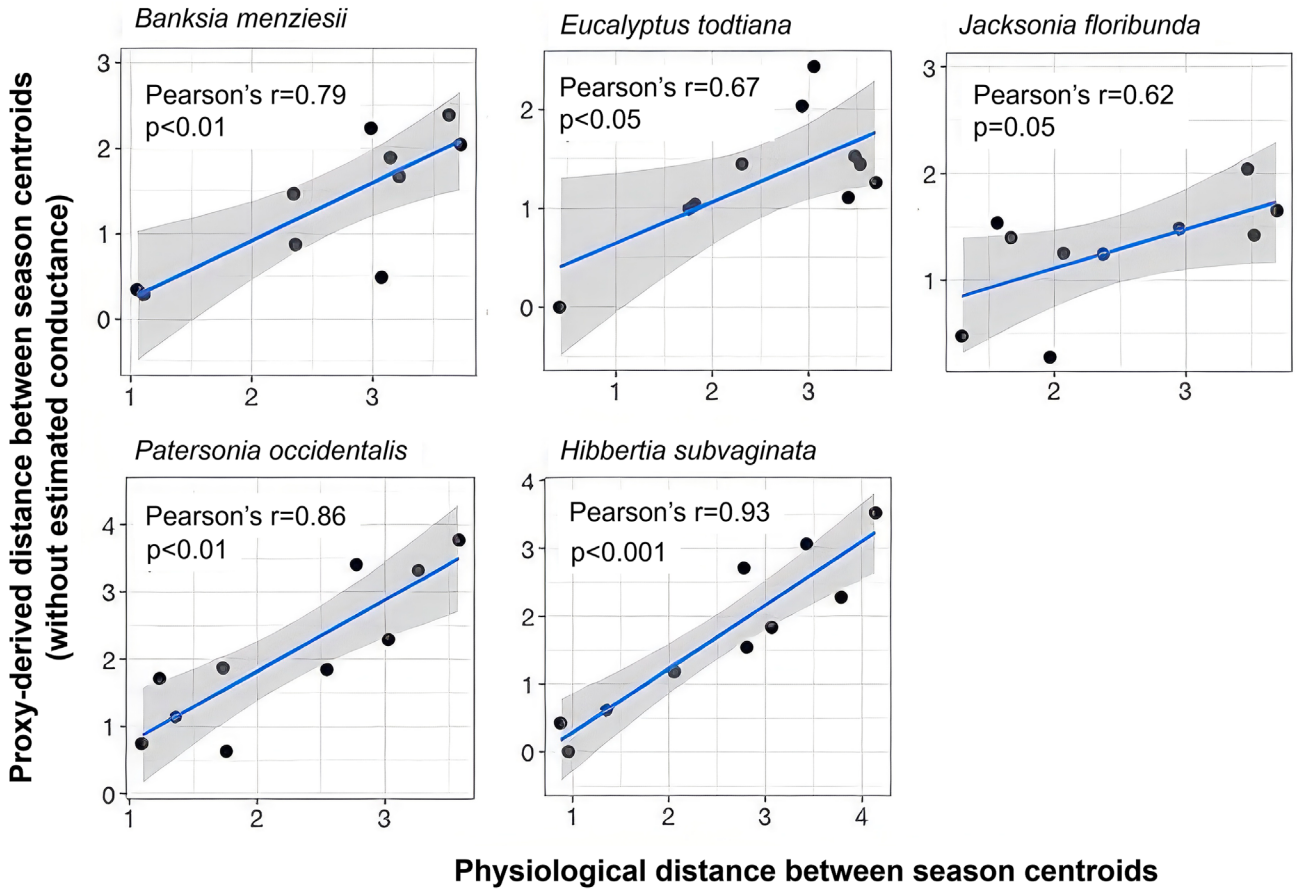

FIGURE 9 Linear regression relationships between physiological distance between season centroids and proxy-derived distance between season centroids (without estimated stomatal conductance) for all studied species. In the scatterplots, Pearson's correlation coefficient (*r*) and *p* values correspond to linear models which relate Euclidean distances between seasons using two different methods are shown and blue line and grey area represents the linear relationship and 95% confidence interval, respectively. Each point in the scatter plot represents a Season 1–Season 2 comparison.

function and leaf morphology) using a single spectral index based in bands within the red edge region.

4.1.4 | Photosynthetic efficiency

The observed relationships between chlorophyll fluorescence-related spectral indices (R_{740}/R_{800} index and the species-specific DPI) and measured *Fv*/*Fm* show promise for the detection of stress-induced loss of photosynthetic efficiency in this functionally diverse plant community. As results were very similar for all our study species, there would seem to be good potential for a wider applicability of proximal sensing for chlorophyll fluorescence across different species in diverse plant communities. Possible improvements to direct fluorescence sensing (and not a related parameter, such as *Fv*/*Fm*) are of great interest to plant condition assessments as they are informative of plant condition across species and functional types. Overall, having a reliable proxy indicator of *Fv*/*Fm* or other fluorescence-related parameters could be of great value for vegetation monitoring due to the transferability of interpretation across different species and its well-known relationship to stress processes (Van Kooten & Snel, 1990).

4.1.5 | Combining proxy-indicators through a multivariate approach

In this study we showed that, when combined, hyperspectral-derived indicators of physiological variables can reliably track seasonal change in plant condition in a very similar way as traditionally measured physiological traits. Importantly, this can be achieved with remotely sensed data extracted from hyperspectral reflectance only, without the need of including estimated stomatal conductance obtained through thermal imagery.

Our multivariate approach to track plant condition using spectral indicators, and its verification using actual physiological measures, expands upon previous approaches. For example, Zinnert et al. (2013) used principal component analysis (PCA) to show that a combination of spectral indices in the red and infra-red regions could differentiate plants that were stressed by natural factors

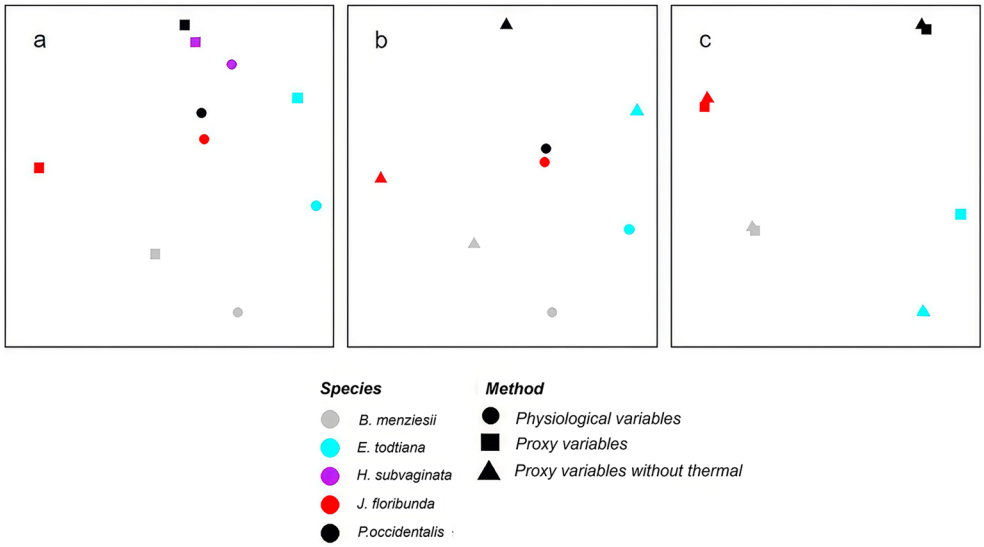

FIGURE 10 Second stage non-metric multi-dimensional scaling between season centroid resemblance matrices using different data sets. (a) Physiological variable data set versus the proxy-derived variable data set using all variables, (b) physiological variable data set versus the proxy-derived variable data set using all variables except estimated stomatal conductance through thermal imagery and (c) proxy-derived variable data set using all variables versus the proxy-derived variable data set using all variables except estimated stomatal conductance through thermal imagery. In these plots, colours represent different species and shapes represent different data sets. The closer two points are to each other, the more similar are the season centroid distance matrices they represent.

(drought and heat) from plants that were stressed by toxic elements in the soil. In contrast, Potts et al. (2006) used several physiological but no spectral variables to characterise the distinct response of two semi-arid grass species to simulated precipitation pulses. Like our study, they used Euclidian distances from their multivariate analysis to track plant responses through time. Although we used Euclidian distances to quantify and visualise seasonal changes in plant condition, this same approach can also be used to present other timelines or contrasts, such as plant condition during successional trajectories, effects of ecosystem disturbances or management interventions. Recently, Wang et al. (2022) used Euclidian distances between species centroids derived from a multivariate analysis of different species spectral information to assess phenological variation. Our approach based on nMDS visualisation and distances between seasonal centroids is simpler, more intuitive and more focused on the condition aspect, rather than on species spectral diversity, although a modified approach to Wang et al. (2022) could possibly be used for the purpose of condition tracking as performed in this study.

Close correspondence between the assessments of plant condition based on proxy versus measured physiological variables suggests that spectral reflectance captured sufficient information for our study species to quantify their distinct responses to seasonal drought and heat stress. These Banksia woodland species experience severe drought and heat stress during summer, but the spectral proxy for stomatal conductance proved non-essential in the multivariate analysis, and the spectral proxies for leaf water status were relatively poor. It would therefore seem that our other proxies correlated sufficiently well with these key water relations variables to reflect that aspect of their response to seasonal stress.

In summary, the method presented in this study represents an alternative to traditional methods when it comes to monitoring plant condition. The multivariate nMDS approach based on spectral traits could be used to establish a 'reference' profile for each species defining expected distances between seasonal centroids. Then, monitoring of plants using the same set of proxy indicators could detect significant deviations from reference values, potentially indicating excessive stress and risk of plant mortality.

5 | CONCLUSIONS

In a complex plant community with a large range of leaf morphologies and adaptations to drought stress, we explored the use of remotely sensed proxy indicators to understand plant condition change. We showed that remotely sensed proxy indicators accurately predicted some physiological variables (e.g. LWC and chlorophyll concentration) in plants of different functional types, whereas lower reliability was found for some other variables (e.g. *Fv*/*Fm* and stomatal conductance). Additionally, we propose an approach that uses multivariate statistics to combine remotely-sensed proxy indicators generated through leaf hyperspectral reflectance data. This allowed us to track plant physiological change with similar accuracy as traditional physiological variables in a plant community with multiple leaf morphologies and different adaptations to environmental change. In the context of ecological restoration, this approach could be used to evaluate restoration success more efficiently, identify optimal restoration methods and inform adaptive management, thereby improving long-term restoration outcomes. Further research will be needed to validate the approach in different ecological settings, and to investigate upscaling

to remote sensing to enable large-scale mapping of plant condition. Nonetheless, we have demonstrated the great potential of hyperspectral data for evaluating plant condition in a functionally and morphologically diverse plant community.

AUTHOR CONTRIBUTIONS

Jaume Ruscalleda-Alvarez, Justin M. Valliere, Victoria Marchesini, Jason C. Stevens, Jean W. H. Yong and Erik Veneklaas conceived the ideas and designed methodology; Jaume Ruscalleda-Alvarez and Victoria Marchesini collected the data; Jaume Ruscalleda-Alvarez analysed the data; Jaume Ruscalleda-Alvarez, Erik Veneklaas and Justin M. Valliere led the writing of the manuscript. All authors contributed critically to the drafts and gave final approval for publication.

ACKNOWLEDGEMENTS

This research was funded by the Centre for Mine Site Restoration, through the Australian Research Council Industrial Transformation Training Centre for Mining Restoration (ARC Project ICI150100041) and supported by an Australian Government Research Training Program (RTP). We thank Wei San Wong, Rodrigo Pires, Fiamma Riviera and Dylan Gibson for their support in data collection. V.M. also acknowledges the support of the Argentinian National Research Sciences Council (CONICET) in the form of a travel grant.

CONFLICT OF INTEREST STATEMENT

The authors declare that they have no known competing financial interests or personal relationships that could have appeared to influence the work reported in this paper.

PEER REVIEW

The peer review history for this article is available at https://www.webofscience.com/api/gateway/wos/peer-review/10.1002/2688-8319.70195.

DATA AVAILABILITY STATEMENT

All data used for this study are available at https://doi.org/10.5061/dryad.4qrfj6qr3.

ORCID

Jaume Ruscalleda-Alvarez https://orcid.org/0000-0001-8365-2239
Justin M. Valliere https://orcid.org/0000-0003-3599-2911
Jean W. H. Yong https://orcid.org/0000-0003-3325-8254
Erik Veneklaas https://orcid.org/0000-0002-7030-4056

REFERENCES

Asner, G. P., Ustin, S. L., Townsend, P. A., Martin, R. E., & Chadwick, K. D. (2024). Forest biophysical and biochemical properties from hyperspectral and LiDAR remote sensing. In *Remote Sensing Handbook, Volume IV* (pp. 96–124). CRC Press.

Bellon-Maurel, V., Fernandez-Ahumada, E., Palagos, B., Roger, J.-M., & McBratney, A. (2010). Critical review of chemometric indicators commonly used for assessing the quality of the prediction of soil attributes by NIR spectroscopy. *TrAC, Trends in Analytical Chemistry*, *29*(9), 1073–1081.

Blackburn, G. A. (2006). Hyperspectral remote sensing of plant pigments. *Journal of Experimental Botany*, *58*(4), 855–867. https://doi.org/10.1093/jxb/erl123

Cao, Z., Wang, Q., & Zheng, C. (2015). Best hyperspectral indices for tracing leaf water status as determined from leaf dehydration experiments. *Ecological Indicators*, *54*, 96–107. https://doi.org/10.1016/j.ecolind.2015.02.027

Clarke, K. R., Tweedley, J. R., & Valesini, F. J. (2014). Simple shade plots aid better long-term choices of data pre-treatment in multivariate assemblage studies. *Journal of the Marine Biological Association of the United Kingdom*, *94*(1), 1–16.

Clevers, J. G. P. W., Kooistra, L., & Schaepman, M. E. (2008). Using spectral information from the NIR water absorption features for the retrieval of canopy water content. *International Journal of Applied Earth Observation and Geoinformation*, *10*(3), 388–397. https://doi.org/10.1016/j.jag.2008.03.003

Clevers, J. G. P. W., Kooistra, L., & Schaepman, M. E. (2010). Estimating canopy water content using hyperspectral remote sensing data. *International Journal of Applied Earth Observation and Geoinformation*, *12*(2), 119–125. https://doi.org/10.1016/j.jag.2010.01.007

Curran, P. J. (1989). Remote sensing of foliar chemistry. *Remote Sensing of Environment*, *30*(3), 271–278.

Dobrowski, S., Pushnik, J., Zarcotejada, P., & Ustin, S. (2005). Simple reflectance indices track heat and water stress-induced changes in steady-state chlorophyll fluorescence at the canopy scale. *Remote Sensing of Environment*, *97*(3), 403–414.

Feng, L., Chen, S., Zhang, C., Zhang, Y., & He, Y. (2021). A comprehensive review on recent applications of unmanned aerial vehicle remote sensing with various sensors for high-throughput plant phenotyping. *Computers and Electronics in Agriculture*, *182*, 106033. https://doi.org/10.1016/j.compag.2021.106033

Filella, I., & Penuelas, J. (1994). The red edge position and shape as indicators of plant chlorophyll content, biomass and hydric status. *International Journal of Remote Sensing*, *15*(7), 1459–1470.

Fu, Y., Yang, G., Pu, R., Li, Z., Li, H., Xu, X., Song, X., Yang, X., & Zhao, C. (2021). An overview of crop nitrogen status assessment using hyperspectral remote sensing: Current status and perspectives. *European Journal of Agronomy*, *124*, 126241. https://doi.org/10.1016/j.eja.2021.126241

Gould, K. S., Markham, K. R., Smith, R. H., & Goris, J. J. (2000). Functional role of anthocyanins in the leaves of *Quintinia serrata* A. Cunn. *Journal of Experimental Botany*, *51*, 1107–1115.

Hendry, G. A., & Grime, J. P. (1993). *Methods in comparative plant ecology: A laboratory manual*. Springer Science & Business Media.

Jones, H. G. (1999b). Use of thermography for quantitative studies of spatial and temporal variation of stomatal conductance over leaf surfaces. *Plant, Cell & Environment*, *22*(9), 1043–1055. https://doi.org/10.1046/j.1365-3040.1999.00468.x

Jones, H. G. (2014). *Plants and microclimate: A quantitative approach to environmental plant physiology* (3rd ed.). Cambridge University Press.

Jones, H. G. (1999a). Use of infrared thermometry for estimation of stomatal conductance as a possible aid to irrigation scheduling. *Agricultural and Forest Meteorology*, *95*(3), 139–149.

Lambers, H., Chapin, F. S., & Pons, T. L. (2008). *Plant physiological ecology*. Springer.

Lehnert, L. W., Meyer, H., Obermeier, W. A., Silva, B., Regeling, B., & Bendix, J. (2018). *Hyperspectral data analysis in R: The hsdar package*. https://doi.org/10.48550/ARXIV.1805.05090

Leinonen, I., Grant, O. M., Tagliavia, C. P., Chaves, M. M., & Jones, H. G. (2006). Estimating stomatal conductance with thermal imagery. *Plant, Cell & Environment*, *29*(8), 1508–1518.

Lu, J., Wu, Y., Liu, H., Gou, T., Zhao, S., Chen, F., Jiang, J., Chen, S., Fang, W., & Guan, Z. (2024). Estimation of plant water content in

cut chrysanthemum using leaf-based hyperspectral reflectance. *Scientia Horticulturae*, *323*, 112517.

Maes, W. H., & Steppe, K. (2012). Estimating evapotranspiration and drought stress with ground-based thermal remote sensing in agriculture: A review. *Journal of Experimental Botany*, *63*(13), 4671–4712. https://doi.org/10.1093/jxb/ers165

McKenna, P. B., Lechner, A. M., Phinn, S., & Erskine, P. D. (2020). Remote sensing of mine site rehabilitation for ecological outcomes: A global systematic review. *Remote Sensing*, *12*(21), 3535. https://doi.org/10.3390/rs12213535

Monteith, J., & Unsworth, M. (2013). *Principles of environmental physics: Plants, animals, and the atmosphere*. Academic Press.

Pate, J. S., & Beard, J. S. (1984). *Kwongan: Plant life of the sandplain: Biology of a south-west Australian shrubland ecosystem*. University of Western Australia Press.

Pate, J. S., & Bell, T. L. (1999). Application of the ecosystem mimic concept to the species-rich Banksia woodlands of Western Australia. *Agroforestry Systems*, *45*(1/3), 303–341. https://doi.org/10.1023/A:1006218310248

Pearcey, R., Mooney, H. A., & Rundel, P. W. (2012). *Plant physiological ecology: Field methods and instrumentation*. Springer Science & Business Media.

Peñuelas, J., Peñuelas, J., Filella, I., Biel, C., Serrano, L., & Savé, R. (1993). The reflectance at the 950–970 nm region as an indicator of plant water status. *International Journal of Remote Sensing*, *14*(10), 1887–1905.

Potts, D. L., Huxman, T. E., Enquist, B. J., Weltzin, J. F., & Williams, D. G. (2006). Resilience and resistance of ecosystem functional response to a precipitation pulse in a semi-arid grassland. *Journal of Ecology*, *94*(1), 23–30.

R Core Team. (2021). *R: A language and environment for statistical computing*. R Foundation for Statistical Computing. https://www.R-project.org/

Rapaport, T., Hochberg, U., Shoshany, M., Karnieli, A., & Rachmilevitch, S. (2015). Combining leaf physiology, hyperspectral imaging and partial least squares-regression (PLS-R) for grapevine water status assessment. *ISPRS Journal of Photogrammetry and Remote Sensing*, *109*, 88–97. https://doi.org/10.1016/j.isprsjprs.2015.09.003

Ruscalleda-Alvarez, J. (2022). Near-surface remote sensing of plant condition in mine site restoration environments.

Ruscalleda-Alvarez, J. (2026). Spectral, thermal and physiological data used for modeling. *Dryad*. https://doi.org/10.5061/dryad.4qrfj6qr3

Schneider, C. A., Rasband, W. S., & Eliceiri, K. W. (2012). NIH image to ImageJ: 25 years of image analysis. *Nature Methods*, *9*(7), 671–675. https://doi.org/10.1038/nmeth.2089

Serbin, S. P., Singh, A., McNeil, B. E., Kingdon, C. C., & Townsend, P. A. (2014). Spectroscopic determination of leaf morphological and biochemical traits for northern temperate and boreal tree species. *Ecological Applications*, *24*(7), 1651–1669. https://doi.org/10.1890/13-2110.1

Serbin, S. P., & Townsend, P. A. (2020). Scaling functional traits from leaves to canopies. In *Remote sensing of plant biodiversity* (pp. 43–82). Springer.

Siegmann, B., & Jarmer, T. (2015). Comparison of different regression models and validation techniques for the assessment of wheat leaf area index from hyperspectral data. *International Journal of Remote Sensing*, *36*(18), 4519–4534. https://doi.org/10.1080/01431161.2015.1084438

Sims, D. A., & Gamon, J. A. (2003). Estimation of vegetation water content and photosynthetic tissue area from spectral reflectance: A comparison of indices based on liquid water and chlorophyll absorption features. *Remote Sensing of Environment*, *84*(4), 526–537.

Sishodia, R. P., Ray, R. L., & Singh, S. K. (2020). Applications of remote sensing in precision agriculture: A review. *Remote Sensing*, *12*(19), 3136. https://doi.org/10.3390/rs12193136

Tao, H., Xu, S., Tian, Y., Li, Z., Ge, Y., Zhang, J., Wang, Y., Zhou, G., Deng, X., Zhang, Z., Ding, Y., Jiang, D., Guo, Q., & Jin, S. (2022). Proximal and remote sensing in plant phenomics: 20 years of progress, challenges, and perspectives. *Plant Communications*, *3*(6), 100344. https://doi.org/10.1016/j.xplc.2022.100344

Thenkabail, P. S., Lyon, J. G., & Huete, A. (2019). *Hyperspectral remote sensing of vegetation. Volume I, fundamentals, sensor systems, spectral libraries, and data mining for vegetation* (2nd ed.). CRC Press.

Townsend, P. A. (2014). Collaborative research: Dimensions NASA: Linking remotely sensed optical diversity to genetic, phylogenetic and functional diversity to predict ecosystem processes. *Directorate for Biological Sciences*, *13*(1342778), 42778 NSF Award Number 1342778.

Valliere, J. M., Alvarez, J. R., Cross, A. T., Lewandrowski, W., Riviera, F., Stevens, J. C., Tomlinson, S., Tudor, E. P., Wong, W. S., Yong, J. W. H., & Veneklaas, E. J. (2022). Restoration ecophysiology: An ecophysiological approach to improve restoration strategies and outcomes in severely disturbed landscapes. *Restoration Ecology*, *30*(S1), e13571. https://doi.org/10.1111/rec.13571

Van Kooten, O., & Snel, J. F. (1990). The use of chlorophyll fluorescence nomenclature in plant stress physiology. *Photosynthesis Research*, *25*, 147–150.

Vina, A., & Gitelson, A. A. (2011). Sensitivity to foliar anthocyanin content of vegetation indices using green reflectance. *IEEE Geoscience and Remote Sensing Letters*, *8*(3), 464–468. https://doi.org/10.1109/LGRS.2010.2086430

Walker, B., Kinzig, A., & Langridge, J. (1999). Original articles: Plant attribute diversity, resilience, and ecosystem function: The nature and significance of dominant and minor species. *Ecosystems*, *2*(2), 95–113. https://doi.org/10.1007/s100219900062

Wang, R., Gamon, J. A., & Cavender-Bares, J. (2022). Seasonal patterns of spectral diversity at leaf and canopy scales in the Cedar Creek prairie biodiversity experiment. *Remote Sensing of Environment*, *280*, 113169.

Wehrens, R., & Mevik, B.-H. (2007). *The pls package: principal component and partial least squares regression in R*.

Williams, P. (2014). The RPD statistic: A tutorial note. *NIR News*, *25*(1), 22–26.

Zarco-Tejada, P. J., Pushnik, J. C., Dobrowski, S., & Ustin, S. L. (2003). Steady-state chlorophyll a fluorescence detection from canopy derivative reflectance and double-peak red-edge effects. *Remote Sensing of Environment*, *84*(2), 283–294.

Zinnert, J. C., Via, S. M., & Young, D. R. (2013). Distinguishing natural from anthropogenic stress in plants: Physiology, fluorescence and hyperspectral reflectance. *Plant and Soil*, *366*(1–2), 133–141. https://doi.org/10.1007/s11104-012-1414-1

SUPPORTING INFORMATION

Additional supporting information can be found online in the Supporting Information section at the end of this article.

Appendix S1. Figure S1. Thermal image used for estimating stomatal conductance of a leaf of Eucalyptus todtiana growing in a restored mine site. (A) sample leaf on which stomatal conductance was estimated; (B) non-transpiring leaf (achieved through petroleum jelly application) to be used in the dry-reference method (Jones, 1999b); (C) crumbled aluminium foil leaf model to be used in the dry-reference method (Jones, 1999b). (D) Temperature sensor used to calibrate thermal images. See temperature scale at the right of the image.

Appendix S2. Figure S2.1. Change in physiological variables measured throughout the study (September 2018 to December 2019) for all studied species. Each point represents the average value

from all sampled plants of a given species at each of the sampling times. Leaf water potential (LWP); relative water content (RWC); leaf water content (LWC); equivalent water thickness (EWT); maximum quantum efficiency of Photosystem II (*Fv*/*Fm*). For each variable, a mean coefficient of variation (CV = standard deviation/mean) was calculated (based on the CV for the five species): LWP – CV = 0.60 MPa, RWC – CV = 0.16, LWC – CV = 0.13, EWT – CV = 0.24 g cm^{-2}, *Fv*/*Fm* – CV = 0.29, stomatal conductance – CV = 0.77 mol m^{-2} s^{-1}.

Figure S2.2. Change in total chlorophylls, carotenoids and anthocyanins concentration measured throughout the study (September 2018 to December 2019, *x* axis) for all studied species. Each point represents the average value for all sampled plants of a given species at each of the sampling times. For each pigment, a mean coefficient of variation (CV = standard deviation/mean) was calculated (based on the CV for the five species): Total chlorophyll – CV = 0.53 μg cm^{-2}, Carotenoids – CV = 0.46 μg cm^{-2}, Anthocyanins – CV = 0.68 μg cm^{-2}.

Appendix S3: Table S3.1. Spectral band ranges used to generate normalised difference spectral indices (in the form of $(R_1 - R_2)/(R_1 + R_2)$) that best correlate with total area-based chlorophyll content (μg cm^{-2}) in the studied species. When selecting any 1 nm wide spectral band between Band 1 lower and upper ends, and any 1 nm wide spectral band between Band 2 lower and upper ends, to form a normalised difference spectral index with them, the correlation between this index and total chlorophyll content for a given species will have a coefficient of determination (R^2) of at least the value indicated as 90% of maximum R^2.

Table S3.2. Analysis of covariance (ANCOVA) results, testing the significance of the factor *species* on the slope of the relationship Total chlorophyll content and best spectral index $((R_{714} - R_{758})/(R_{714} + R_{758}))$ for all species.

Table S3.3. Maximum coefficients of determination (R^2) between normalised difference spectral indices $((R_1 - R_2)/(R_1 + R_2))$ and carotenoid and anthocyanins leaf content (in μg cm^{-2}), obtained in the optimised spectral index analysis using the visual spectrum (400–800 nm). For each regression, associated *p*-values and the involved narrow spectral bands (R_1 and R_2) are presented.

Appendix S4: Figure S4. Number of plant species for which the studied methods provided accurate levels of prediction (RPD >=2), for different variables related to plant water status and water content. Water status and water content-related variables—LWP: leaf water potential, RWC: relative water content, LWC: leaf water content, EWT: equivalent water thickness. On the *x* axis, spectral analysis method grouping (in brackets) and specific methods used in these groups (represented by individual ticks within each group). From left to right the first five groups represent water absorption features: 650 Abs (650 nm absorption feature), 970 Abs (970 nm absorption feature), 1200 Abs (1200 nm absorption feature), 1450 Abs (1450 nm absorption feature) and 1940 Abs (1940 absorption feature). In each absorption feature there are 3 ticks that indicate 3 different measures: area of the absorption feature, maximum depth of the absorption feature and maximum depth/area of the absorption feature. Der 900–1200 (derivative reflectance features between 900 nm and 1200 nm, which includes, from left to right, the following measures: slope of the spectrum between 900 to 970 nm, 1000 and 1050 nm, 1100 and 1200 nm, and 1200 and 1270 nm), PLSR (partial least square regression using absolute reflectance, using the visible spectrum only (450 to 700 nm), visible and near infra-red spectrum (450 to 950 nm), near infra-red and shortwave infra-red spectrum (700 to 2400 nm) and shortwave infra-red spectrum (950 to 2400 nm)), derPLSR (partial least square regression using derivative reflectance, using the same methods described for absolute reflectance), Opt SI (Optimised Spectral Indices in the form of a normalised difference index, $(R_2 - R_1)/(R_1 + R_2)$, where R_2 and R_1 are two different 1 nm wide wavelengths).

Appendix S5: Table S5.1. PERMANOVA test results for the effect of sampling season on Euclidean distance resemblance matrices of each species studied, using three different data sets (physiological variables, all proxy indicators and proxy indicators without data derived from thermal images). 'Res' stands for residual variation.

Table S5.2. Pairwise PERMANOVA analysis comparing differences between each season, based on Euclidean distance resemblance matrices of each species, using three different data sets (physiological variables, all proxy indicators and proxy indicators without data derived from thermal images). Non-significant differences between seasons are reported as for *p*-values >0.05. *p*-values <0.001 are reported as '***'; *p*-values <0.01 are reported as '**' and *p*-values <0.05 are reported as '*'. 'Negative' indicates no significant difference between seasons. Note seasons are expressed in western standards to facilitate the general reader's understanding.

Table S5.3. Summary of the non-metric multidimensional scaling (nMDS) analysis results. For each species, the most influential variables when separating samples from different seasons are presented. This was done using the physiological data set, the full proxy indicator data set and the proxy indicator data set without estimated conductance. Note that for *H. subvaginata*, the proxy indicator data set without estimated conductance and the full proxy indicator data set are the same, as estimated conductance was removed from the full data set through the variable selection explained in the methods section. Linear regression coefficients of determination and *p*-values are shown between season centroid distances using different data sets. *Fv*/*Fm*—maximum potential quantum efficiency of Photosystem II, Chls—total chlorophyll concentration, $Chls_e$—chlorophyll spectral index, Fv/Fm_e—spectral index related to maximum potential quantum efficiency of Photosystem II (Double Peak Index), G—stomatal conductance, G_e—estimated stomatal conductance, LWP—leaf water potential, LWC—leaf water content and LWC_e—estimated leaf water content.

Appendix S6: Figure S6. Non-metric multidimensional scaling (nMDS) using Euclidean Distance of physiological (middle) and proxy variable with (top) and without estimated conductance Gs (bottom) for four different plant species (fifth species figure is provided in the main manuscript). Vectors in the bottom right of each sample nMDS plot represent the Pearson correlation of variables explaining the variation. Vector directions and lengths indicate the relative influence of each variable in separating samples within the multi-dimensional

space. Season centroids nMDS were produced from the distance among centroid for each season, calculated from the Euclidean distance resemblances. Scatterplots (right) show the relationship between the Euclidean distances matrices of the seasonal centroids derived from two data sets. In the scatterplots, Pearson's correlation coefficient (*r*) and *p* values corresponding to linear models which relate Euclidean distances between seasons using two different methods are shown and blue line and grey area represents the linear relationship and 95% confidence interval, respectively. Each point in the scatter plot represents a Season 1–Season 2 comparison. LWC—leaf water content; LWCe—estimated leaf water content; Gs—stomatal conductance; Gs_e—estimated stomatal conductance; Chls—total chlorophyll concentration; SI Chl—spectral index related to chlorophyll content; DPI—Double Peak Index, Car—total carotenoids concentration; Anth—total anthocyanin concentration.

Appendix S7: Table S7. Coefficients of determination, root mean square error (RMSE) and wavelengths selected for the formation of an optimised spectral index that would provide the lowest RMSE of linear models predicting a set of water-status-related variables in five different plant species (*Patersonia occidentalus*, *Hibertia subvaginata*, *Jacksonia floribunda*, *Eucalytpus todtiana* and *Banksia menziesii*). Units of RMSE are the following—equivalent water thickness (EWT): g/cm^2, LWC: g/g (proportion from 0 to 1); RWC: g/g (proportion from 0 to 1) and LWP: Mpa.

How to cite this article: Ruscalleda-Alvarez, J., Valliere, J. M., Marchesini, V., Stevens, J. C., Yong, J. W. H., & Veneklaas, E. (2026). Tracking plant condition in a functionally diverse restored plant community through a combination of proxy indicators. *Ecological Solutions and Evidence*, *7*, e70195. https://doi.org/10.1002/2688-8319.70195